Comparison of Seismic Response Calculation Model for Long-span Cable-stayed Bridge on Rock Site

C. Luo[(1)], Y. Li[(2)], H. Wang[(3)], M. Lou[(4)] , S. Liu[(5)]

[(1)] *Lecture, State Key Laboratory of Mechanical Behavior and System Safety of Traffic Engineering Structures, Shijiazhuang Tiedao University, luochao@stdu.edu.cn*
[(2)] *Undergraduate student, Shijiazhuang Tiedao University, 1040774451@qq.com*
[(3)] *Lecture, State Key Laboratory of Mechanical Behavior and System Safety of Traffic Engineering Structures, Shijiazhuang Tiedao University, wanghao@stdu.edu.cn*
[(4)] *Professor, State Key Laboratory of Disaster Reduction in Civil Engineering, Tongji University, lml@tongji.edu.cn*
[(5)]*Associate Professor, School of Civil Engineering and Architecture, Zhejiang Sci-tech University, sliu_2008@163.com*

Abstract

To discuss soil-structure interaction(SSI) effect and site effect to a long span cable-stayed bridge, three models in computing seismic response are compared. They are (1) structure model with uniform excitation, (2) structure model with multiple support excitation and (3) seismic SSI model. The bridge has a total length of 1457m and is divided into six spans of 78m, 145m, 860m, 285m and 89m. The local site of the bridge is a rock site. The shear wave velocity of the surface layer of the site is 3408m/s. The local site of the bridge has significant terrain fluctuations, and the deepest and the shallowest height difference is 175m.

Based on the response spectrum of the site, an artificial seismic wave can be obtained as the uniform excitation for the structure model. The seismic motions for multiple supported excitation which consider the site effects are obtained by a 2D site response analysis. In site response analysis, a so-called mix-boundary method proposed by the author is used to consider the difference in height between the left and right boundaries. The bedrock wave for site response analysis is obtained by deconvolution. With 600m depth of the deconvolution and site response model, the multiple support excitation for the second model is calculated. For the SSI model, a full 3D bridge-foundation-rock model is built. The model also has a depth of 600m. Similarly, the mix-boundary method and the same bedrock motion in model (2) are used. The 3D model has 512880 nodes, 522071 elements and 1160745 degrees of freedom.

Base on the three models above, the seismic response of the long span cable-stayed bridge is compared, and some useful conclusions can be concluded. Firstly, the site effect has a great influence on the seismic response of the bridge, and it mainly reflects on the low frequency components. The maximum relative errors of displacement and internal force responses by ignoring site effects are 44.84% and 65.51%, respectively. By neglecting the site effect, the seismic response of the structural response could be greatly underestimated. Moreover, the SSI effect has a relatively small influence, and it mainly reflects on a frequency of 0.55Hz. The maximum relative errors of displacement and internal force responses by ignoring SSI effects are 14.03% and 11.22%, respectively. Furthermore, the SSI effect also leads to the long period oscillation of internal force response after the peak response appears, which could have a great influence which considering the nonlinearity of material. In practice, the site effect cannot be neglected, and the SSI effect should be taken into consideration as much as possible.

Keywords: site effect; soil-structure interaction; multiple support excitation; cable-stayed bridge.

1. Introduction

In the seismic design of long-span bridges, the calculation model of input ground motion has an important influence on seismic response. For long-span bridges, the input methods of ground motion generally are uniform excitation, multi-support excitation, and inputting bedrock motion to the overall soil-structure model by considering SSI. When taken the SSI into account, there are many simplified models such as the spring model[1], lumped-mass model[2], and p-y spring model[3]. These simplified models greatly simplify the calculation of SSI problems. However, simplifications often lead to computational errors. Generally, it is more precise and reliable by considering soil and structure as a whole system, but this method usually consumes more time and computing resources. Nowadays, with the improvement of the computing ability of computers, a large amount of literature has adopted the soil-structure integral finite element model to calculate the seismic response of long-span bridges considering SSI[4-7]. However, the sites where long-span bridges are located in these works of literature are soft soil sites. There is currently little literature discussing SSI on bedrock sites. Some scholars[8, 9] believe that the SSI effect on the bedrock site is weak, and the rigid foundation model can be used to effectively calculate the seismic response of the structure on the bedrock site. However, among them, the group pile foundation is simplified as the impedance function. Therefore, it is necessary to establish an integral soil-structure finite element model to consider SSI and to discuss the rationality of various calculation models for large-span bridges on the bedrock site. In this paper, A comparison of three different models in computing seismic response of this bridge will be presented, and the site effects and SSI effect on the seismic response of a long span cable-stayed bridge will be discussed.

2. Engineering details of the prototype

The long span cable-stayed bridge selected in this paper is the Guanshan bridge. Guanshan bridge is a cross-sea bridge in Zhoushan, Zhejiang province, China. The profile of the cable-stayed bridge and site is shown in Fig. 1.

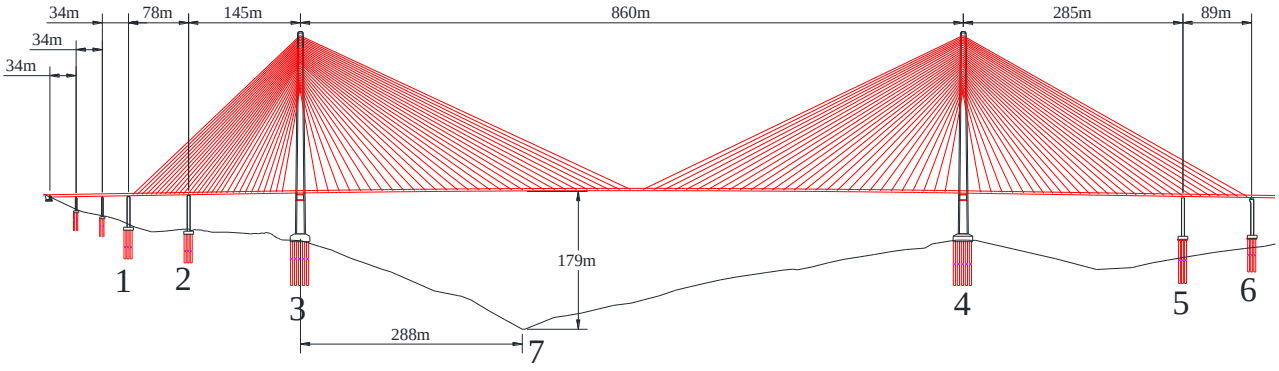

Fig. 1 Profile of cable-stayed bridge and site

2.1 local site conditions

It can be seen from Fig. 1 that the terrain is undulating within the project site area. When determining the time history of the acceleration of the bedrock surface, the terrain topography and the dynamic parameters of the rock mass should be considered. According to the drilling records, the material parameters of the bedrock at different depths can be determined. Table 1 shows the elastic material parameters of the rock layer along the depth direction.

From Table 1, the layer at a depth of 48m has much less shear wave velocity that other layers. This layer is a weak interlayer.

Table 1 elastic material properties of rock site

Depth(m)	Shear wave velocity(m/s^2)	Density(kg/m^3)	Passion ratio	Damping ratio
2	3408	2500	0.23	0.03
3	3318	2500	0.23	0.03
4	3028	2500	0.23	0.03
5	3249	2500	0.23	0.03
6	3353	2500	0.23	0.03
7	2957	2500	0.23	0.03
8	3199	2500	0.23	0.03
9	2985	2500	0.23	0.03
10	3446	2500	0.23	0.03
11	3446	2500	0.23	0.03
12	3849	2500	0.23	0.03
13	3873	2500	0.23	0.03
14	3897	2500	0.23	0.03
15	4023	2500	0.23	0.03
16	3151	2500	0.23	0.03
17	3504	2500	0.23	0.03
18	3390	2500	0.23	0.03
19	3826	2500	0.23	0.03
20	3997	2500	0.23	0.03
22	3891	2500	0.23	0.03
24	3779	2500	0.23	0.03
26	3465	2500	0.23	0.03
28	3504	2500	0.23	0.03
30	3484	2500	0.23	0.03
32	3427	2500	0.23	0.03
34	3408	2500	0.23	0.03
36	3336	2500	0.23	0.03
38	3584	2500	0.23	0.03
40	3626	2500	0.23	0.03
42	3167	2500	0.23	0.03
44	3849	2500	0.23	0.03
46	3922	2500	0.23	0.03
48	1049	2000	0.23	0.05
50	3965	2500	0.23	0.03
inf	4200	2600	0.23	0.02

2.2 Details of the bridge

The span combination of the Guanshan bridge is 78m + 145m + 860m + 285m + 89m, which is shown in Fig. 1. The section of the steel box girder is shown in Fig. 2. Fig. 3 shows the main tower structure of the cable-stayed bridge. Cable-stayed bridges are composed of three kinds of materials: concrete, steel, and steel strands. The material properties can be found in Table 2. Given the effect of the sag of the cable due to its gravity, a reduction of Young's modulus of the cable should be considered by the Ernst equation as follows:

$$E_{eff} = \frac{E}{1+\frac{q^2 S^2 A \cos^2 \alpha}{12T^3}E} \quad (1)$$

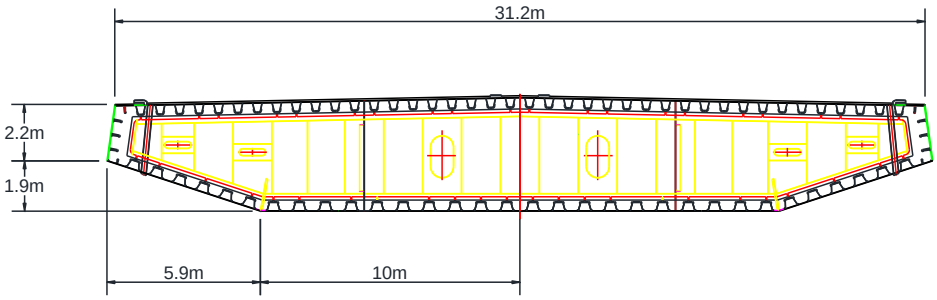

Fig. 2 section of steel box girder

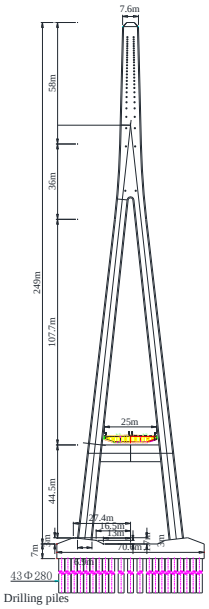

Fig. 3 Schematic diagram of the main tower structure and position of cables

Table 2 Material properties of Guanshan bridge

	Young's modulus(Pa)	Possion ratio	Density (kg/m^3)	part
Concrete	3×10^{10}	0.2	2300	Main tower, pier and cap
Steel	2.1×10^{11}	0.3	7850	Girder
Steel strand	3×10^{11}	0.2	7850	Cable

In this paper, all the materials are assumed to be linear elastic. More details of the Guanshan bridge can be found in [10].

3. Numerical Simulation

3.1 Input motion

An artificial bedrock motion from the report of seismic safety evaluation for engineering site(SSEES) is chosen in this paper. The time history, FFT and response spectrum plots of the motion are shown in Fig. 4. Since the site of Guanshan bridge is rock site, this bedrock motion is the motion at the ground surface. This motion does not consider the site effect and does not have the characteristics of spatial variability. It can only be used for uniform excitation of the bridge. The input motion multiple supported excitation model and SSI model will be introduced in section 3.2 and 3.3.

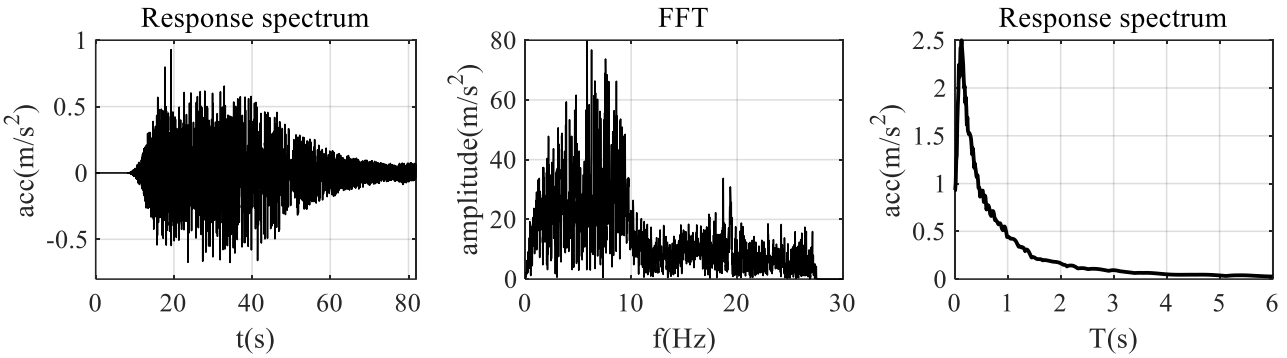

Fig. 4 Artificial Bedrock motion in SSEES

3.2 Modelling

The structural system of the Guanshan bridge is a floating system. To consider the SSI effect and site effect, three finite element models are established according to the parameters of the rock site and bridge structure mentioned in the previous section:

(1) The rock site model, which is shown in Fig. 5. This model is used to calculate the input ground motion with spatial variability considering the local site effects.

(2) The finite element model of the Guanshan bridge, which is used to calculate the seismic response with uniform excitation and multiple support excitation.

(3) The SSI model, which is used to calculate seismic response considering SSI.

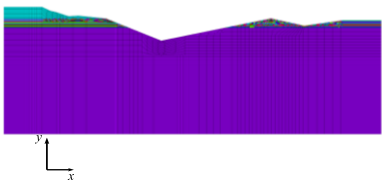

Fig. 5 Rock site model

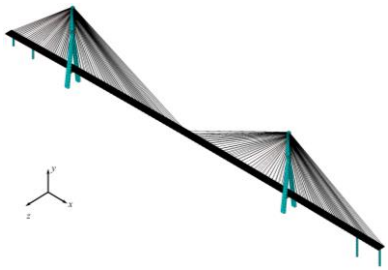

Fig. 6 Guanshan bridge model

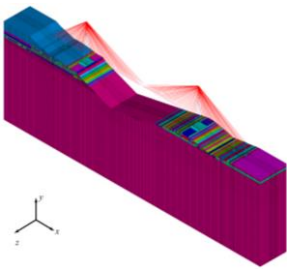

Fig. 7 SSI model

In the rock site model, the rock layers are modeled using the four-node plane elements. The main towers, girders, piers and beams of in the Guanshan bridge model and the SSI model are modeled with beam elements. In the SSI model, eight-node solid element is used to model the pile caps and the rock site. In wave propagation problems, the accuracy of numerical simulation depending on mesh size of the finite element model and time step of time history. Kuhlemeyer et al. [11]indicateds that a rational mesh size required 8 nodes per wavelength for a given frequency. The rational mesh size can be calculated as the equations below:

$$\Delta h \le \frac{\lambda_{\min}}{8} = \frac{Cs}{8 f_{\max}} \tag{2}$$

In this paper, the maximum frequency of interest is 27.5Hz, which can be seen from Fig. 4. According to the data in Table 1, the corresponding rational mesh size of each layer can be calculated. In transient analysis, follow the similar requirements, the maximum time step should satisfy the requirement that 16-time steps per period for a given frequency, then a rational time step can be calculated as follows:

$$\Delta t \le \frac{1}{16 f_{\max}} \tag{3}$$

In this paper, the maximum frequency of interest is f=27.5Hz, then $\Delta t \approx 0.0023$. For the convenience of interpolation for the original records, Δt=0.002 is used in this paper.

3.3 Deconvolution and site response analysis

In this section, the input motion of multiple support excitation considering site effect will be calculated. As mentioned before, the SSEES bedrock motion can only be used for uniform excitation. The site effects can be considered through a site response analysis for the rock site model. Before performing the site response analysis, the input motion of the rock site model and SSI model should be determined. As the motion introduced in section 3.1 is the motion at the ground surface, it is necessary to conducting a 1D deconvolution to calculate the input motion at the bottom depth of the rock site model. Luo[10] has mentioned that for the site of Guanshan bridge, the depth of the rock site model is directly related to the accuracy of numerical results, and a depth of 600m is adequate for the Guanshan bridge site. More details can be found in literature [10].

In this paper, the left bank rock layer parameters of the site are selected as the 1D deconvolution model. The 1D deconvolution is conducted in the frequency domain by using finite element methods. The viscous boundary[12] is applied at the bottom and the calculation of equivalent load follows the procedure in Joyner's method[13]. The verification of this deconvolution procedure and more detail can be found in literature [10]. Fig. 8 shows the velocity time history of outcrop motion at the depth of 600m, which is the input motion of the rock site model and SSI model.

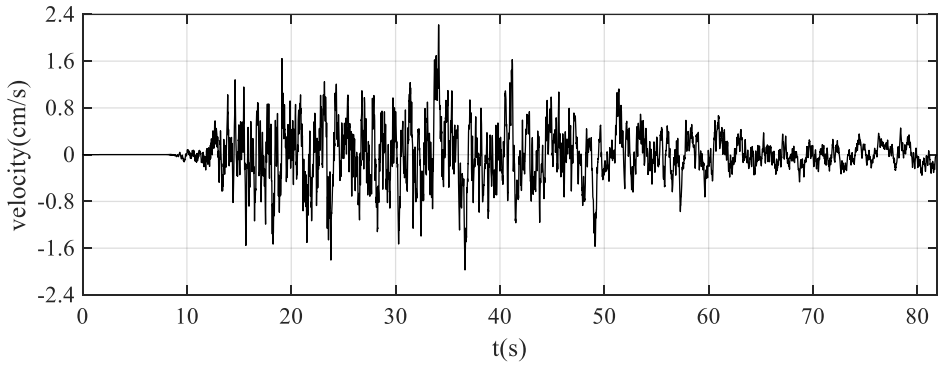

Fig. 8 Velocity time history of outcrop bedrock motion at the depth of 600m

In site response analysis, the viscous-spring boundary[14] is installed at the bottom and lateral boundary, the Modified Domain Reduction Method[15] is applied in calculating the equivalent forces of the model. Free field motions for Modified Domain Reduction Method were developed from 1D wave propagation analysis.

Through the site response analysis, the acceleration time history response at observation points showed in Fig. 1 can be calculated. Table 3 shows the horizontal and vertical PGA results at each observation point. The maximum and minimum PGA in the horizontal direction are at observations 4 and 7, respectively, and The maximum and minimum PGA in the vertical direction are at observations 3 and 7, respectively. In the horizontal direction, only observations 5 and 7 have a lower PGA than the SSEES bedrock motion. It is worth noting that the other five observation points are all at the pier position.

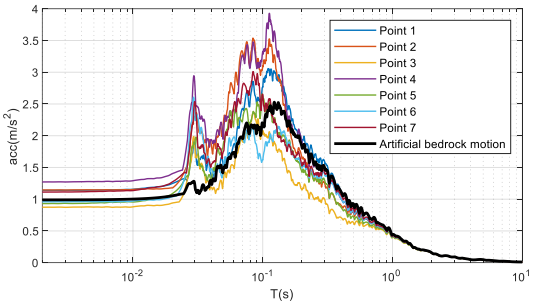

Fig. 9 Response spectrum of horizontal acceleration at each observation points and artificial bedrock motion

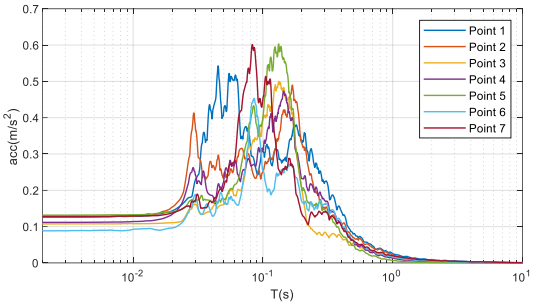

Fig. 10 Response spectrum of vertical acceleration at each observation points

Table 3 PGA at each observation points

Observation Points	PGA-Horizontal(m/s^2)	PGA-Vertical(m/s^2)
1	1.030	0.112
2	1.127	0.180
3	1.159	0.135
4	1.276	0.110
5	0.976	0.111
6	1.115	0.133
7	0.877	0.105
SSEES bedrock motion	0.989	0

3.4 Analysis cases

To measure the site effects and SSI effects on the seismic response of the Guanshan Bridge. The seismic response of the Guanshan bridge will be calculated following the cases shown in Table 4. In case 1 and case 2, the bridge model shown in Fig. 6 is adopted. The input motion of case 1 is the SSEES bedrock motion in SSEES shown in Fig. 4. As described in Section 3.3, Case 2 uses the result of the site response analysis as the input ground motion. The direct method[16] is adopted as the input method of multiple support excitation in case 2. In case 3, the 600m depth outcrop bedrock motion is adopted as input motion, along with the Modified Domain Reduction method as the seismic wave input method.

Table 4 Analysis cases

Case	Model	Input motion
1	Bridge model	Uniform excitation Artificial bedrock motion
2	Bridge model	Multiple support excitation Ground motion from site response analysis
3	SSI model	600m depth outcrop bedrock motion

3.4 High-performance computing platform

All the analysis cases are computed in the “Chao compute” platform in this paper. As mentioned before, the SSI model has 512880 nodes, 522071 elements and 1160745 degrees of freedom. The transient analysis has 40960 time steps. For most of the commercial and open-source FEM software on PC, this task can hardly be done. To improve computational efficiency, the Chao compute platform based on MATLAB has been developed. The Chao compute platform integrates the functions of the Modified Domain Reduction Method, iterative solver and HDF5 data format, which improves the efficiency in computing greatly. For example, on

a computer processor with single-core clocked at 2.6GHZ and 64G memory, a comparison of the computing speed of the different model by different software is shown below:

Table 5 Execution time and speedup ratio of analysis for different models

Model	Degree of freedom (DOF)	Total time of 40960 steps analysis		Speedup ratio
		Ansys	Chao compute	
Rock site model	110,014	16.6 hours	3.6 hours	4.56
SSI model	1,160,745	250 hours	31.5 hours	7.93

For both the rock site model and the SSI model, the Chao compute shows much better efficiency than that of the commercial software in linear transient analyses.

4. Numerical results

To compare the seismic response of long-span cable-stayed bridges under the three different cases, the relative displacement between the top and bottom of the two main towers(RDT), the relative displacements at the joints between the girder and the towers(RDJ), and the bending moments(BMT), shear forces(SFT), axial forces(AFT) at the bottoms of the main towers were selected for comparison. By assuming case 3 as the exact solution, the peak response of each case and errors of case 1 and case 2 are shown in Table 6. Due to space limitations, only the time history and Fourier spectrum of the left main tower are plotted. Fig. 11 to Fig. 15 show the time history of RDT, RDJ, BMT, AFT and SFT. Due to the difference between the three computation cases, the results show different characteristics, and the results will be discussed in the following four aspects.

Table 6 Peak response of three cases and relative error of case 1 and case 2

Peak response		Case 1	Case 1 error (%)	Case 2	Case 2 error (%)	Case 3
Left main tower	RDT(cm)	1.31	**-37.30**	2.00	**-4.10**	2.08
	RDJ(cm)	1.22	**-36.75**	2.09	**8.29**	1.93
	BMT (10^3×kN•m)	1.11	**-57.56**	2.90	**11.22**	2.60
	SFT (10^3×kN)	51.98	**-31.68**	73.15	**-3.86**	76.08
	AFT(10^3×kN)	2.86	**5.05**	2.47	**-9.24**	2.72
Right main tower	RDT(cm)	1.07	**-44.84**	1.89	**-2.41**	1.94
	RDJ(cm)	1.25	**-30.64**	2.05	**14.03**	1.80
	BMT (10^3×kN•m)	0.82	**-65.51**	2.52	**6.09**	2.38
	SFT (10^3×kN)	55.07	**-24.78**	72.67	**-0.73**	73.21
	AFT(10^3×kN)	2.93	**-4.92**	3.01	**-2.36**	3.08

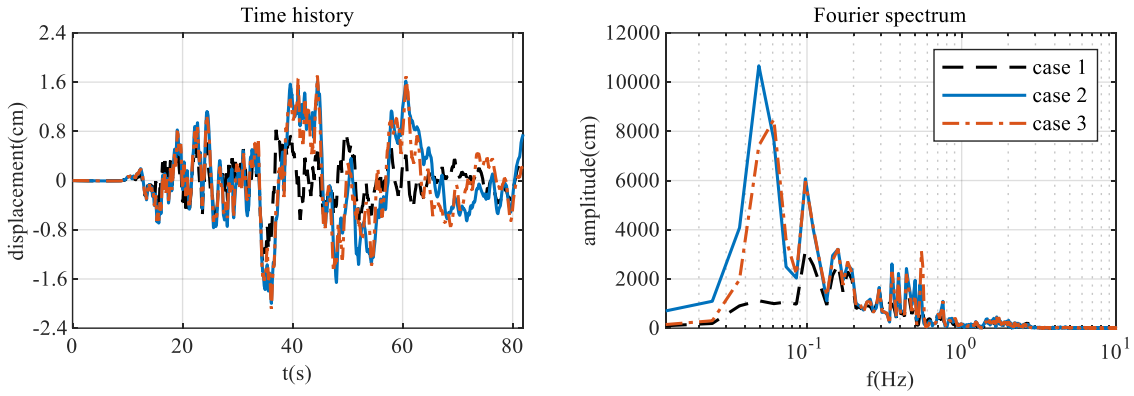

Fig. 11 RDT of Left tower

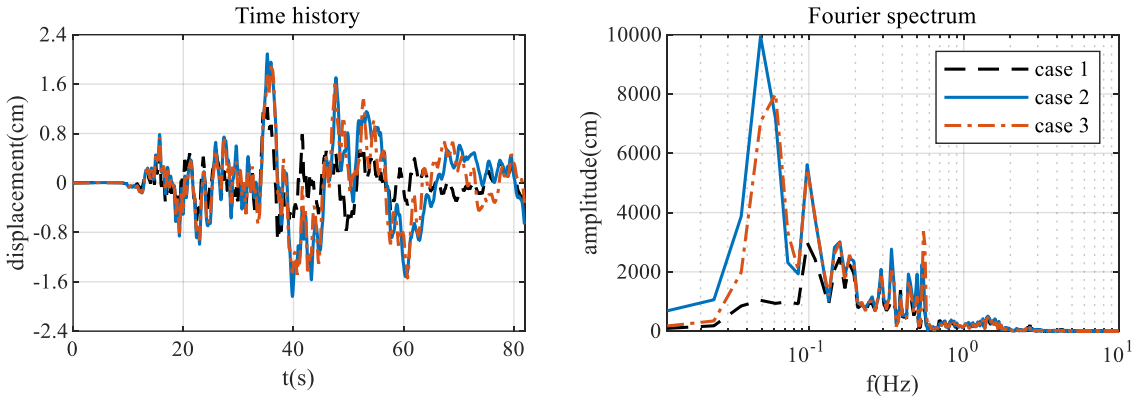

Fig. 12 RDJ of Left tower

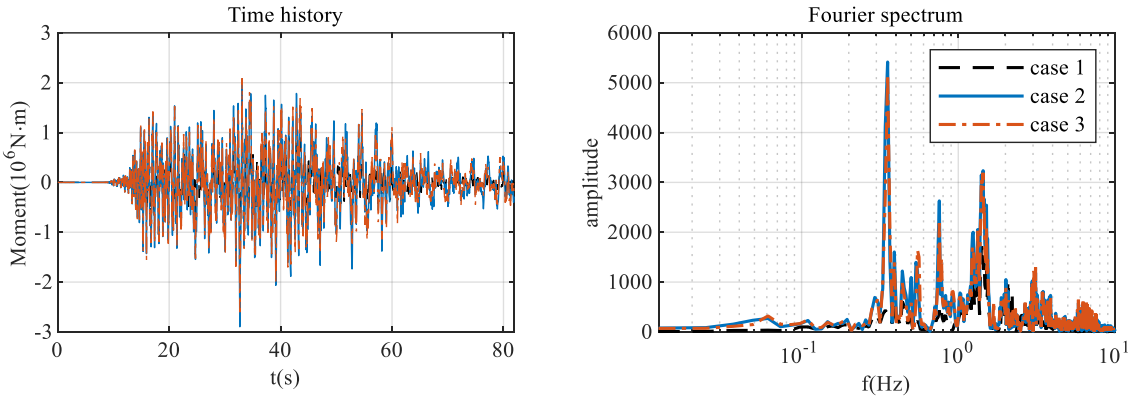

Fig. 13 BMT of Left tower

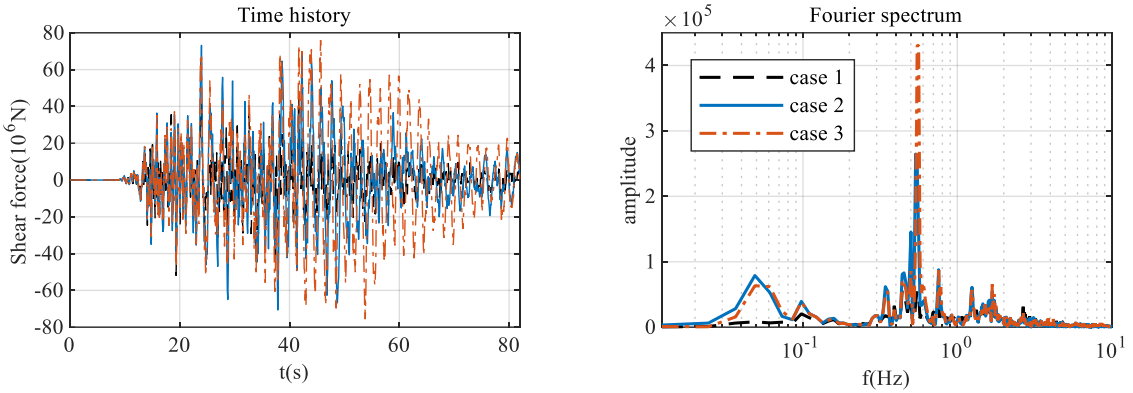

Fig. 14 SFT of Left tower

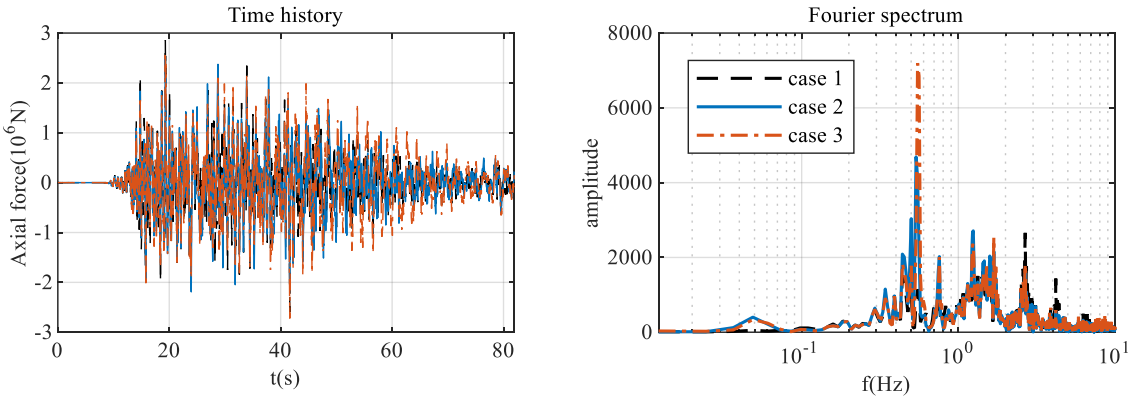

Fig. 15 AFT of Left tower

4.1 Displacement response

From Table 6, the results of case 1 have a much smaller displacement amplitude than that of case 2 and case 3. For the results of case 1 and case 2, their maximum errors are 44.84% and 14.03%, respectively. The time history and FFT plots of RDT and RDJ of the three cases are shown in Fig. 11 and Fig. 12. From the time history response, the consistency of the waveform of case 2 with case 3 is better than case 1. The FFT plots show that the main difference between the three cases is concentrated in low frequency. Case 1 has a much smaller amplitude than case 2 and case 3 at a frequency range of 0-2Hz. Case 2 has a higher amplitude than case 3 at a frequency range of 0-0.06Hz and lower amplitude than case 3 at a frequency range of 0.06-0.09Hz and 0.4-0.6Hz.

4.2 Internal force response

From Table 6, the results of case 1 also have a much smaller internal force amplitude than that of case 2 and case 3. For the results of case 1 and case 2, their maximum errors are 65.51% and 11.22%, respectively. The time history and FFT plots of BMT, AFT and SFT among the three cases are shown from Fig. 13 to Fig. 15. For the bending moment response, the consistency of the waveform of case 2 with case 3 is better than case 1, while for the shear force and axial force response, neither of case 1 and case 2 has good consistency of waveform with case 3. The FFT plots show that the main difference between the three cases is concentrated in difference frequency range with the displacement response. For the bending moment response, the amplitude of case 1 is smaller than that of case 3 in almost all frequency ranges, only except for 0.2-0.25 Hz, while case 2 has good agreement with case 3 on the whole 0-10Hz frequency ranges. For the shear force and axial force response, neither of case 1 and case 2 has good consistency of waveform with case 3. For shear force response, the main difference between case 1 and case 3 in frequency components concentrated on

0.03-0.15Hz and 0.3-0.8Hz, and case 2 has a much higher amplitude than case 3 in 0.5-06Hz. For the axial force response, case 1 has a lower amplitude in 0.04-0.08Hz and 0.5-0.8Hz and high amplitude in 2.5-4.5Hz than case 3. Similar to the shear force, the results of case 2 in axial force also have much higher amplitude than case 3 in 0.5-0.6Hz.

4.3 Site effect

By comparing the results of case 1 and case 2, the influence of site effect on the Guanshan bridge can be evaluated. From the discussion above, it is clear that case 1 has much smaller peak response on displacement and internal force results. The maximum error of displacement and internal force response of case 1 are 44.84% and 65.51%, respectively. For an engineering site like the Guanshan bridge site, the site effect cannot be neglected.

4.4 SSI effect

By comparing the results of case 2 and case 3, the influence of the SSI effect on the Guanshan bridge can be evaluated. From the peak response aspect, the influence of the SSI effect is not much, since the maximum error for displacement and internal force response of case 2 are 14.03% and 8.29%, respectively. While when comparing the whole time history and FFT plots of shear force and axial force, neglecting the SSI effect will significantly change the waveform and frequency components of the results. For both the shear force and axial force results, case 3 has much higher amplitude results than case 2 at a frequency of about 0.55Hz, which leads to much higher amplitude from 40-80s in the time domain. In practice, the influence of the SSI effect on time history waveform and frequency components could have more influence than the bridge project discussed in this paper, especially when considering the nonlinearity of material. It is necessary to take the SSI effect into account in practice as much as possible.

5. Conclusion

In this paper, to evaluate the site effect and SSI effect to the seismic response to a long span cable-stayed bridge, three computation model was established. They are the uniform excitation model, the multiple support excitation model and the SSI model. The input motion of the multiple support excitation model is calculated by a site response analysis. By comparing the displacement and internal force response of the three models, some useful conclusions can be summarised.

1. For displacement response, ignoring site effects can cause errors of more than 30%. By ignoring the SSI effect, errors of more than 10% may occur. These errors are mainly reflected in the low frequency part of the structural response.
2. For internal force response, ignoring site effects can cause errors of more than 60%. These errors are mainly concentrated in low frequency range. By ignoring the SSI effect, errors of more than 10% may occur, and these errors are mainly displayed in the frequency of 0.55Hz.
3. For the long span cable-stayed bridge located on a rock site, the site effect has more significant influence on the structural response than the SSI effect. By neglecting the site effect, the seismic response of the bridge could be greatly underestimated.
4. Though on the rock site, the SSI effect also has a significant influence on the structural response. Besides over 10% error of peak response, the SSI effect also leads to the long period oscillation of internal force response after the peak response appears, which could have a great influence which considering the nonlinearity of material.

5. Acknowledgements

This work presented was sponsored by the National Natural Science Foundation of China under Grant numbers 91315301 and 51808500, Natural Science Foundation of Hebei Province under Grant numbers E2019210350 and E2019210245, the project for the introduction of overseas students in Hebei Province

under Grant numbers C20190363 and C20190364,and State Key Laboratory of Mechanical Behavior and System Safety of Traffic Engineering Structures under Grant number ZZ2020-04, These supports are gratefully acknowledged.

5. Copyrights

6. References

[1] Penzien J, Scheffey C F, Parmelee R A (1964): Seismic analysis of bridges on long pile. *Journal of the Engineering Mechanics Division*, **90** (3), 223-254.

[2] Sun L, Zhang C, Pan L, et al (2002): Lumped-mass Model and Its Parameters for Dynamic Analysis of Bridge Pier-pile-soil System. *Journal of Tongji University (natural science)*, **30** (4), 409-415.

[3] Boulanger R W, Curras C J, Kutter B L, et al (1999): Seismic soil-pile-structure interaction experiments and analyses. *Journal of Geotechnical and Geoenvironmental Engineering*, **125** (9), 750-759.

[4] Jeremić B, Kunnath S, Xiong F (2004): Influence of soil – foundation – structure interaction on seismic response of the I-880 viaduct. *Engineering Structures*, **26** (3), 391-402.

[5] Elgamal A, Yan L, Yang Z, et al (2008): Three-dimensional seismic response of humboldt bay bridge-foundation-ground system. *Journal of Structural Engineering-ASCE*, **134** (7), 1165-1176.

[6] Jeremić B, Jie G, Preisig M, et al (2009): Time domain simulation of soil-foundation-structure interaction in non-uniform soils. *Earthquake Engineering & Structural Dynamics*, **38** (5), 699-718.

[7] Gu Y, Fu C C, Aggour M S (2016): Topographic Effect on Seismic Response of a High-Pier Bridge Subjected to Oblique Incidence Waves. *Developments in International Bridge Engineering: Selected Papers from Istanbul Bridge Conference 2014*. Springer International Publishing. Cham:Springer International Publishing, 2016, 165-174.

[8] Stewart J P, Fenves G L, Seed R B (1999): Seismic soil-structure interaction in buildings. I: Analytical methods. *Journal of Geotechnical and Geoenvironmental Engineering*, **125** (1), 26-37.

[9] Stewart J P, Seed R B, Fenves G L (1999): Seismic soil-structure interaction in buildings. II: Empirical findings. *Journal of Geotechnical and Geoenvironmental Engineering*, **125** (1), 38-48.

[10] Luo C (2017): *On Effect of River Valley Topography and Soil-structure Interaction for Seismic Response of Long-span Bridges*. Shanghai: Tongji University.

[11] Kuhlemeyer R L, Lysmer J (1973): Finite element method accuracy for wave propagation problems. *Journal of the Soil Mechanics and Foundations Division*, **99** (5), 421-427.

[12] Lysmer J, Kuhlemeyer R L (1969): Finite dynamic model for infinite media. *Journal of the Engineering Mechanics Division*, **95** (4), 859-878.

[13] Joyner W B, Chen A T (1975): Calculation of nonlinear ground response in earthquakes. *Bulletin of the Seismological Society of America*, **65** (5), 1315-1336.

[14] Liu J, Du Y, Du X, et al (2006): 3D viscous-spring artificial boundary in time domain. *Earthquake Engineering and Engineering Vibration*, **5** (1), 93-102.

[15] Luo C, Lou M, Gui G, et al (2019): A modified domain reduction method for numerical simulation of wave propagation in localized regions. *Earthquake Engineering and Engineering Vibration*, **18** (1), 35-52.

[16] Luo C, Lou M, Gui G (2015): Comparison for Calculation Methods of Long span Structure under Multi support Seismic Excitation. *Journal of Tongji University (natural science)*, **43** (1), 8-15.

